2023 IEEE International Conference on Robotics and Automation (ICRA 2023)
May 29 - June 2, 2023. London, UK

Safe Operations of an Aerial Swarm via a Cobot Human Swarm Interface

Sydrak S. Abdi[1] and Derek A. Paley[2]

Abstract— **Command and control of an aerial swarm is a complex task. This task increases in difficulty when the flight volume is restricted and the swarm and operator inhabit the same workspace. This work presents a novel method for interacting with and controlling a swarm of quadrotors in a confined space. EMG-based gesture control is used to control the position, orientation, and density of the swarm. Inter-agent as well as agent-operator collisions are prevented through a velocity controller based on a distance-based potential function. State feedback is relayed to the operator via a vibrotactile haptic vest. This cobot human swarm interface prioritizes operator safety while reducing the cognitive load during control of a cobot swarm. This work demonstrates that an operator can safely and intuitively control a swarm of aerial robots in the same workspace.**

I. INTRODUCTION

Swarm robotics is an emergent field. Applications in this field range from agriculture [1] and material transport [2], to search and rescue [3] and entertainment [4]. Regardless of the task at hand, the operator is responsible for making sure that the behavior of the swarm is in accordance with the given objectives. As the tasks become increasingly complicated and operators become more involved, it becomes especially important to consider factors that affect the interaction between the operator and the swarm. By reducing the cognitive load on the operator, they may be able to make more informed decisions, leading to more effective and efficient interactions.

The field of human-swarm interactions explores the interface between human operators and robotic swarms in an effort to optimize control over the swarm while reducing the cognitive load on an operator. A cobot, or collaborative robot, is a robot intended to interact with humans within a shared environment. This paper describes a novel cobot human swarm interface (HSI) that reduces cognitive load on the operator by addressing one of the largest hurdles in collaborative robotics, agent-operator collision. The safety of the operator is prioritized and encoded into each agent through the use of distance-based potentials, where as motion and gesture controls relay desired commands and control of an aerial swarm.

Gesture and motion controls are effective methods of relaying an operator's intent to robotic systems. Not only are gestures natural and intuitive means of communication, but machine-learning algorithms have bridged the gap allowing operators to use gestures to communicate with, command, and control robotic systems.

[5], [6], and [7] describe vision-based gesture control methods in which convolutional neural networks classify gestures made by the operator. Once classified, these gestures are translated into control signals and sent to their robotic systems. [8] and [9] extend this idea to multi-agent systems by enabling agents to classify gestures onboard and perform the assigned tasks defined by those gestures autonomously. One downfall to these methods is that they require line of sight to the operator to receive the intended instructions.

Another method of relaying desired commands is through the use of muscle and motion sensing devices such as the Mbientlab IMU bracelet, Myo armband, or OYMotion gForcePro+. [10] presents a method for controlling the 3D position of a quadrotor by confining the motion of the quadrotor to a 3D surface. The position of the quadrotor is determined by finding the intersection between that surface and a pointing vector generated from the arm of the operator wearing an IMU. An external button is used to iterate between predefined surfaces to achieve the desired motion in space. [11] describes an interpreter that uses the motions and static gestures of an operator wearing a Myo armband to replace the functionalities of a computer mouse, allowing an operator to control the formation of a swarm by simply drawing the desired formation with their arm. [12] shows that static gestures may be used to interact with a virtual menu, allowing an operator to have access to a library of desired controls through which they may guide a swarm of ground robots through an environment with obstacles. Similarly, [13] develops a clustering algorithm to perform online gesture recognition and showed that an operator wearing a Myo armband may successfully navigate a drone through an obstacle course containing hoops. Others such as [14], [15], and [16] have expanded these control paradigms to develop multi-modal interfaces that include speech as well as motion and gesture control for their multi-agents systems. Motion and gesture controls are used to select the desired agents, where as speech control is used to directly relay the desired commands to those selected agents.

While being able to control a quadrotor is crucial, the information received about the quadrotor and its states can be just as important, allowing an operator to make more informed decisions. In indoor settings, the domain in which robots move may be limited, so operators naturally rely on visual feedback as their main source of information pertaining to a robot's states. While this is generally sufficient, it becomes increasingly more difficult to estimate these parameters in multi-agent systems or environments that include obstacles.

One method to relay pertinent information quickly is through the use of haptic devices. Intensity, duration, rhythm, and tactor locations are all parameters that can be varied

to develop a library of haptic patterns to relay desired information to an operator. [17] and [18] utilize an Omega 3 active force feedback device as both a joystick and tool to provide haptic feedback. As the Omega teleoperates a swarm of aerial vehicles, resistive force feedback is provided to the operator during flight when the selected direction of travel is impeded by an obstacle, aiding the operator in navigating the swarm around obstacles in the environment. [19] presents a haptic glove paired with six tactors that corresponded to the axes of motion of a teleoperated quadrotor. The tactors on the glove vibrate with varying intensities in proportion to the quadrotor's proximity to any obstacles, providing spatial awareness even when the quadrotor moved directly out of the operator's line of sight. Others have developed libraries of vibrotactile patterns that relayed changes in robotic system's states such as the density and center of mass of a swarm of aerial robots [20] or the attitude of a virtual aircraft [21]. While these works show the benefits of using muscle and motion control sensors as pipelines to provide robotic systems with their operator's intent or desired controls, they are limited to teleportation applications, that is, they lack the ability to allow the operator to directly and safely interact with these robotic systems.

Artificial potential fields and barrier functions have a rich history of being used in path planning and collision avoidance applications for autonomous systems. [22], [23], and [24] successfully developed a steering-based collision avoidance method for vehicles by virtually attaching a variety of velocity potential functions to objects detected in the surrounding environment. The aggregate of the surrounding velocity fields is used to safely steer the car around obstacles. [25] and [26] apply potential fields to the problems of multi-agent path planning through obstacle rich complex environments. [27], [28] and [29] utilize potential fields and barrier functions, respectively, to ensure inter-agent collision avoidance during completion of tasks assigned to the multi-agent systems. The swarm-velocity controller presented here leverages these works to develop a potential based approach that achieves online inter-agent safety as well as operator collision avoidance, while continuously attempting to maintain the prescribed formation.

The contributions of this paper are as follows: (1) a human swarm interface that prioritizes operator safety through the use of distance-based potential functions and feedback control and (2) a gesture-based control methodology that provides an operator with control of a swarm's position, orientation, and density in either the global frame or the operator's body frame. The HSI prevents collisions between the vehicles and the operator, allowing the operator to focus their efforts on completing their tasks rather than their personal safety.

The remainder of this paper is organized as follows. Section II presents experimental preliminaries required to understand the presented work. Section III delves into the control strategies employed, and Section IV reports the experimental results. The conclusions and future work are discussed in Section V.

II. BACKGROUND

The HSI described below is comprised of three distinct pieces of hardware: an EMG-based gesture recognition armband used by the operator to provide desired commands and controls, an aerial swarm of homogeneous miniature quadrotors, and a haptic vest used to provide continuous feedback to the operator.

Electromyography (EMG) sensors measure and record the electrical signals generated in muscles during contraction [30]. The OYMotion gForcePro+ armband is a wearable EMG based gesture recognition device shown in Fig. 1a. Containing an 8-channel EMG array and a 9-axis IMU, the gForcePro+ provides a real-time orientation estimation of the operators forearm as well as gesture recognition via Bluetooth BLE 4.2 up to a range of 10m. Gesture recognition is accomplished utilizing a trainable AI model onboard the armband that allows for up to 16 unique user-defined gestures [31].

The Bitcraze Loco Swarm [32] is an aerial robotic swarm consisting of homogeneous quadrotors called Crazyflies [33] utilizing the Loco Positioning system for localization. Crazyflies, shown in Fig. 1b, are miniature quadrotors measuring 92mm $\times$ 92mm with a takeoff weight of 27g. The Loco Positioning system is an Ultra Wide Band radio based localization system used to find the 3D position of the Crazyflies in space [34]. Loco Positioning nodes [35] are positioned within a room. For this work, these nodes were used to define a flight volume for the swarm. Each Crazyflie is paired with a Loco Positioning deck [36]. High frequency radio messages are sent back and forth between the nodes and the decks, allowing the system to measure the distance between each node and the deck to calculate the position of the deck and therefore the Crazyflie. Position estimation is performed onboard the Crazyflie and sent to the ground station. The Loco Swarm was flown using Crazyswarm, a system architecture for controlling multiple Crazyflies simultaneously [37].

The bHaptics TactSuit X40 is a virtual reality haptic vest, shown in Fig. 1c. Weighing 1.7kg, this haptic vest contains 40 vibrotactile motors, 20 on both the front and back, and is connected to the base station using BLE 4.0. [38].

(a) (b) (c)

Fig. 1: (a) OYMotion gForcePro+, (b) Bitcraze Crazyflie 2.1, (c) bHaptics TactSuit X40

III. CONTROL STRATEGY

In the control strategy described here, the operator utilizes gestures to command and control the position, orientation, and density of the aerial swarm. This is accomplished by dynamically modifying the formation defining the swarm, while each agent autonomously follows their assigned goal positions within the formation.

A. Swarming Formations

The swarming formations used in this work are shown in Fig. 2. All formations are radially symmetric, which is a property that is leveraged when controlling the density of the swarm. While the desired formation is determined by the number of desired agents and a desired radius, no agent is assigned a specific location within the formation. During assembly, the assignment problem is solved using a Munkres assignment algorithm [39], minimizing the distance each agent has to travel to complete the formation.

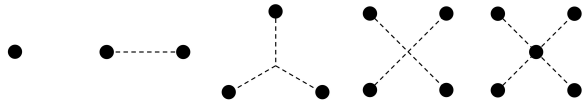

(a) (b) (c) (d) (e)

Fig. 2: Swarming formations per number of agents, ranging from (a-e) 1-5 agents respectively.

B. Gesture Recognition

One of the objectives of this work is to provide an operator with the capability to control the position, orientation, and density of an aerial swarm in both the global frame as well as the operator's body frame. This is achieved using the trained gestures shown in Fig. 3.

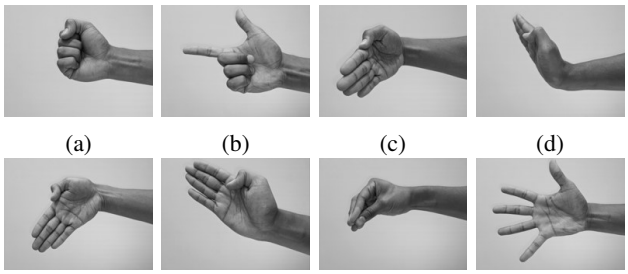

(a) (b) (c) (d)

(e) (f) (g) (h)

Fig. 3: 8 custom gestures recognized by the gForcePro+ AI model after training: (a) closed fist, (b) finger pointing, (c) wrist flexion, (d) wrist extension, (e) ulnar deviation, (f) radial deviation, (g) finger pinch, and (h) finger spread.

Inspired by the work presented in [40] and [41], the selected gestures have been shown to be successfully recognized with a high degree of accuracy using a number of methods, including those employed on the OYMotion gForcePro+. The *closed fist* gesture is assigned the role of commanding the agents to takeoff from their respective locations, as well as assembling the agents into formation. The *finger pointing* gesture lands the aerial swarm. The *wrist flexion* and *wrist extension* gestures give the operator positional control over the swarm. The positional control shown in this work is limited to translation along the X-axis of the inertial frame. This could be extended with 2 additional pairs of gestures to control the translation in the remaining two axes. The *ulnar deviation* and *radial deviation* gestures provide the operator with control of the orientation of the swarm by rotating the swarm counterclockwise and clockwise in the X-Y plane respectively. The *finger pinch* and *finger spread* gestures allow the operator to decrease and increase the density of the swarm respectively.

Gestures were selected as the control modality for this work due to the decrease in the amount of required infrastructure in comparison to tablets or hardware-based control systems, and their lack of ambiguity in comparison to speech-based control systems. The goal of this work is to develop an HSI that prioritizes operator safety, while reducing cognitive load during control of a cobot swarm. One method to decrease the cognitive load on the operator is to decrease the amount of infrastructure the operator is required to engage with.

C. Swarm Velocity Control

Given a swarm of n identical agents, a velocity control algorithm is developed to safely navigate agents from their current locations x, to their goal locations x_g, while circumventing the p obstacles in the environment. The attractive potential $U_{i_{attr}}$ and velocity controller $V_{i_{attr}}$ for agent i can thus be expressed as

$$U_{i_{attr}}(x_i) = V_0||x_i - x_{i_g}|| \tag{1}$$

and

$$\begin{aligned} V_{i_{attr}}(x_i) &= -\nabla U_{i_{attr}}(x_i) \\ &= -\nabla V_0||x_i - x_{i_g}|| \\ &= -V_0\frac{(x_i - x_{i_g})}{||x_i - x_{i_g}||} \end{aligned} \tag{2}$$

where V_o is the desired constant velocity.

The obstacle-avoidance velocity controller was designed to allow agents to safely avoid obstacles while moving towards their goal. The FIRAS function proposed by Khatib [42] is frequently used as a repulsive potential function:

$$U_{obs}(x) = \begin{cases} \frac{1}{2}\eta\left(\frac{1}{\rho} - \frac{1}{\rho_0}\right)^2, & \rho \leq \rho_0 \\ 0, & \rho > \rho_0, \end{cases} \tag{3}$$

where ρ_0 represents the limit distance, or radius of influence, of the repulsive field and ρ represents the shortest distance to the obstacle. This function has been adapted for this applications. The obstacle-avoidance velocity controller $V_{i_{obs}}$

for agent i can thus be expressed as

$$V_{i_{obs}}(x_i) = -\sum_{m=1}^{p} \nabla U_{i_{obs}}(x_i) = \begin{cases} \sum_{m=1}^{p} \eta \left(\frac{1}{\rho_m} - \frac{1}{\rho_0}\right) \frac{1}{\rho_m^2} \frac{\partial \rho_m}{\partial x}, & \rho_m \leq \rho_0 \\ 0, & \rho > \rho_0, \end{cases} \tag{4}$$

where $\rho_m = ||x_i - x_{obs_m}||$ is the distance to obstacle m.

D. Haptic Feedback

The bHaptics TactSuit X40 is a virtual reality haptic vest shown in Fig. 1c. In this work, these motors provide the operator with the continuous location of the center of mass of the swarm with respect to the flight volume. The flight volume was divided into 40 bins, paralleling the motors on the vest. The centroid of the swarm is calculated and localized to 1 of these 40 bins. While the center of mass is in a given bin, the corresponding tactor vibrates on the vest; as the center of mass moves, the analogous motors on the vest vibrate, providing the operator with the continuous spatial awareness of the swarm's location relative to the flight volume and its boundaries in real time. An example of this feedback can be seen in Fig. 4.

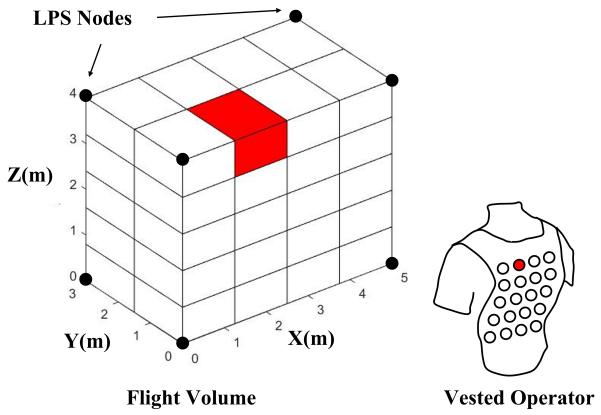

Fig. 4: Experimental setup showing the flight volume defined by the Loco Position system (LPS) Nodes, the bin partitioning utilized to localize the swarm's centroid, and the vested operator receiving haptic feedback regarding the location of the centroid of the swarm.

IV. EXPERIMENTAL RESULTS

Experiments are conducted to demonstrate the gesture-based control methodology in controlling the position, orientation, and density of the swarm in both the inertial frame as well as the operator's body frame, and validate the utility of the designed swarm velocity controller in maintaining operator safety during control of a cobot swarm while occupying the same workspace. All gesture training and experiments were conducted by the authors.

A. Experimental Setup

The system shown in these results is a Loco Swarm using Crazyswarm's *goTo()* functionality in which waypoints are sent to each agent at 4Hz and an onboard controller plans a smooth trajectory from the current state to the waypoint position. The waypoints, $x_{i_{k+1}}$, are derived as shown below:

$$x_{i_{k+1}} = \begin{cases} x_{i_k} + V_{i_{attr}}(x_{i_k})\Delta t + V_{i_{obs}}(x_{i_k})\Delta t, \\ \qquad ||x_{i_k} - x_{i_g}|| > V_{i_{attr}}(x_{i_k})\Delta t \\ x_{i_g} + V_{i_{obs}}(x_{i_k})\Delta t, \\ \qquad ||x_{i_k} - x_{i_g}|| \leq V_{i_{attr}}(x_{i_k})\Delta t, \end{cases} \tag{5}$$

where x_{i_k} is the current position of agent i, $V_{i_{attr}}(x_{i_k})$ are the goal-bound velocities, $V_{i_{obs}}(x_{i_k})$ are the collision avoidance velocities, and Δt is the inverse of the desired waypoint frequency. All positions derived using this methodology are 2-D positions spanning the X-Y plane, with a fixed altitude of 1m in an effort to avoid the effects of the downwash interaction between the aerial agents in the swarm. The prescribed formation has a radius of 0.75m. To ensure inter-agent collision avoidance, the agents in the swarm consider their counterparts obstacles. Fig. 4 shows the experimental setup. For video results refer to supplemental materials shown here: https://youtu.be/9kladblLRj8

B. Position Control in Inertial Frame

In the first experiment, the ability to control the position, orientation, and density of a robotic swarm containing 5 agents through the developed HSI is illustrated. The positional control over the swarm using the *wrist flexion* and *wrist extension* gestures was mapped to a translation of 1m. The *ulnar deviation* and *radial deviation* gestures were mapped to rotations of 22.5°. The *finger pinch* and *finger spread* gestures were mapped to radial translations of 0.25m about the centroid of the Loco Swarm's formation. The operator remained stationary throughout this experiment. Fig. 5 shows a time series of the Loco Swarm's trajectory, as seen from above, during a gesture-based flight demonstration. As shown, an operator can control the position, orientation, and density of a swarm in the inertial frame.

C. Position Control in Operator Frame

The second experiment continued to utilize gesture control. A VICON Vantage V8 system with 12 cameras was used to localize the operator within the environment. During this experiment, the operator was free to move throughout the environment as they desired. A robotic swarm containing 3 agents was localized using the Loco Positioning system. The OYMotion gForcePro+ provides the orientation of operator's arm. Once the pose of the operator's arm is established, a pointing ray from the operator's arm is generated, and the intersection between that ray and the floor may be calculated. The operator then utilizes the previous translational control gestures to relay the intersection point to the Loco Swarm as the desired location for the centroid of the formation. During this control modality, the translational gestures are referred to as *call gestures*. Fig. 6 shows a time series of

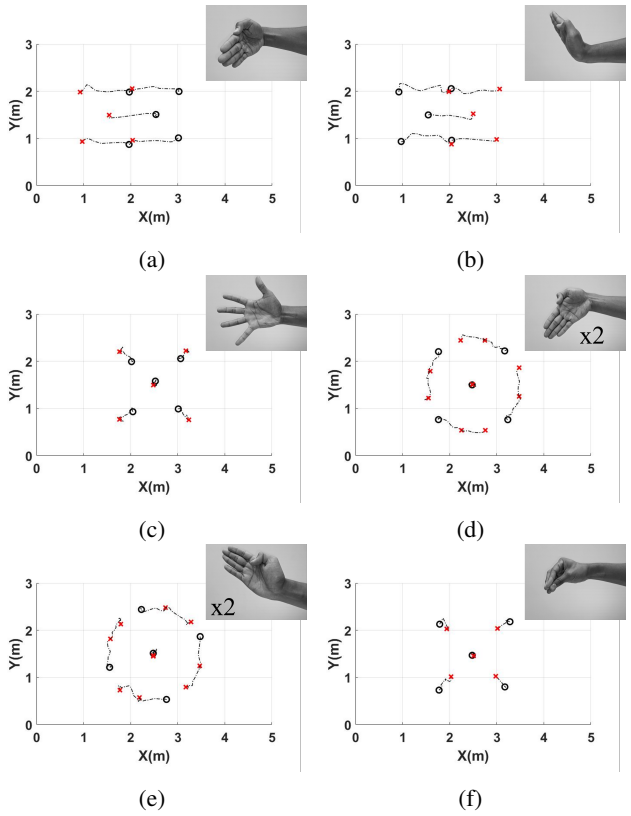

Fig. 5: Time series (a-f) of the Loco Swarm's X-Y trajectory during a gesture based flight demonstration. The locations denoted with the ○ and × symbols represent the initial and final positions of the swarm respectively, before and after each gesture was performed.

the Loco Swarm's and operator's trajectory, as seen from above, during this flight demonstration. As shown, regardless of their movement, an operator can successfully control the position of a swarm in their body frame.

D. Operator Collision Avoidance

The third experiment demonstrates the collision avoidance capabilities of the HSI. The operator is once again localized in the flight volume via the VICON system. Once localized, the position of the operator is added to the list of obstacles. The 3 agents were assigned an avoidance radii of 0.25m and the operator was assigned an avoidance radius of 1m. Fig. 7 shows the minimum, maximum, and average inter-agent distances during this experiment, as well as the inter-agent distance prescribed by the formation. The formation is assigned a radius of 0.75m leading to a prescribed inter-agent distance of approximately 1.3m. At 115*s* into this experiment, the operator decreased the density of the swarm by increasing the formation radius from 0.75m to 1m, leading to a prescribed inter-agent distance of approximately 1.73m. The periods of time near 55*s*, 80*s*, and 115*s* show windows where the operator was not within collision range of the swarm. As shown, the lines converge, since the minimum distance, maximum distance, and average distance between

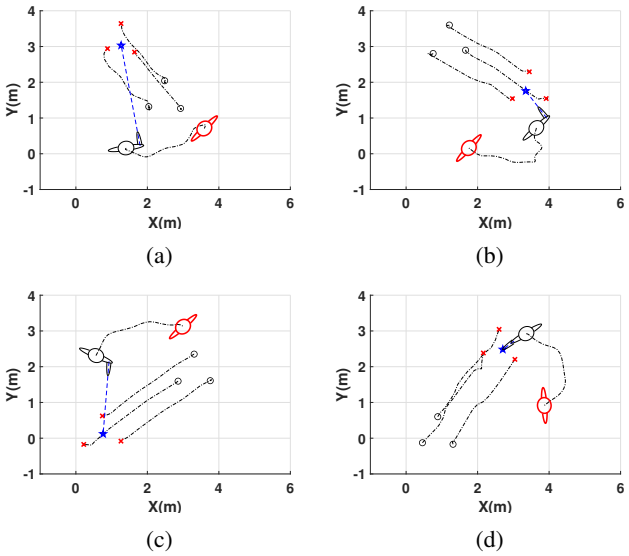

Fig. 6: Time series (a-d) of the operator and Loco Swarm's X-Y trajectory during a flight demonstration utilizing positional control in the operator frame. The locations denoted with the ○ and × symbols represent the initial and final positions of the swarm respectively, before and after the call gesture was performed. The ⋆ symbol denotes the commanded intersection or call point.

agents are all equivalent for the assigned radially symmetric three-agent formation. This plot also shows that as the operator moves back and forth through the swarm, the agents at no point in time collided with each other and respect their assigned avoidance radii.

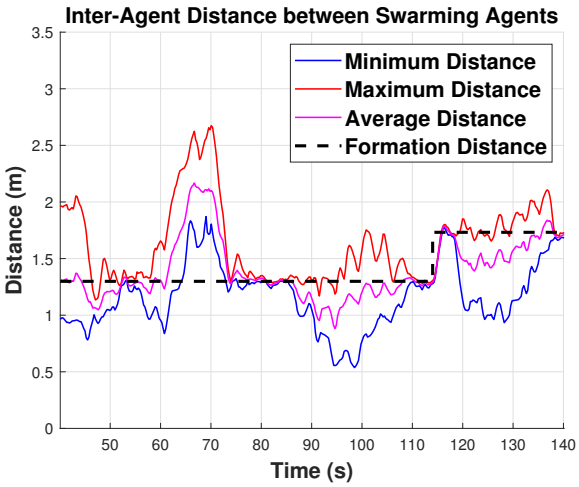

Fig. 7: Time series showing the minimum, maximum, average, and formation based inter-agent distance during operator collision avoidance experiment.

Fig. 8 shows the distance between the operator and the agents within the swarm during the same experiment. From this graph, we can see that during the experiment, the agents avoided collision with the operator, respecting the

operator's designated boundary. Fig. 9 shows a time series of the Loco Swarm avoiding collision with the operator as the operator walks through the center of the flight volume. For a short window beginning at 60*s*, the operator moves forward quickly, forcing the Agent 1 to enter the operator's avoidance radius as can be seen in Fig. 9b and Fig. 9c. Agent 1 quickly compensates and exits the operator's avoidance radius in an effort to maintain desired distances between the obstacles. Thus, as the operator moves from one end of the flight volume to the other, the designed swarm velocity controller allows the Loco Swarm to actively avoid collision with all obstacles, which now include the operator, ensuring the operator's safety during control of a cobot swarm while occupying the same workspace. The operator still maintains control of the aerial swarm via the previously discussed gesture controls as can be seen at the end of the supplemental material.

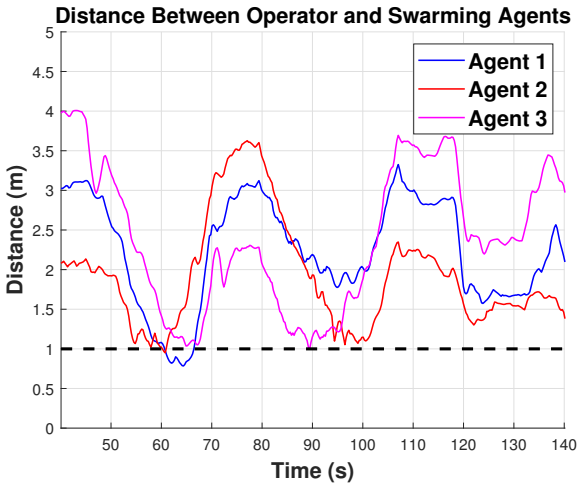

Fig. 8: Time series of the distance between each agent and the operator during operator collision avoidance experiment.

V. CONCLUSION

This work presents a novel cobot human swarm interface (HSI) that prioritizes operator safety while reducing the cognitive load during control of a cobot swarm. The cognitive load required to control a single drone in the presence of a human occupying a confined space is quite high. This load is magnified significantly by increasing the number of aerial vehicles being controlled. The HSI uses EMG-based gesture control to command the position, orientation, and density of the swarm in both the inertial frame, as well as the operator's frame, removing the necessity of controlling multiple agents individually through the use of swarm formation control. The location of the centroid of the swarm is relayed to the operator via a vibrotactile haptic vest. Inter-agent as well as agent-operator collisions are prevented through a swarm velocity controller utilizing a distance-based potential function.

Experimental results demonstrate that an operator can control an aerial swarm while safely occupying and moving throughout the same workspace. Quantification of cognitive loads is a worthwhile endeavour for subsequent research. Ongoing and future work is focused on adapting this HSI to more computationally capable autonomous quadrotors, with an eye towards eliminating the requirement for infrastructure such as the motion capture system for operator localization and laptop base station.

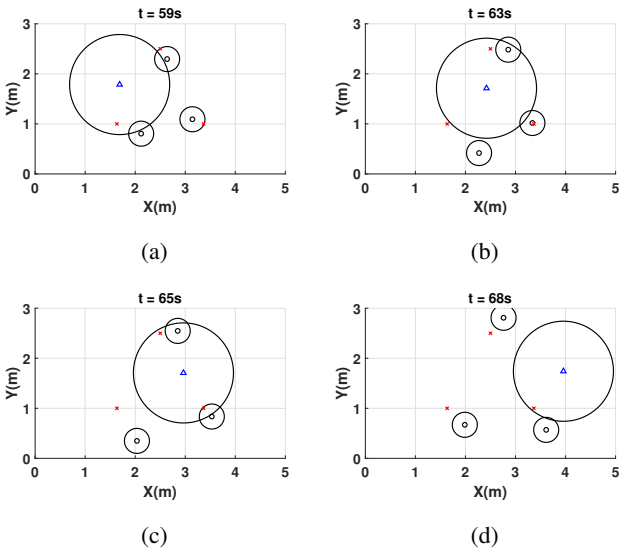

Fig. 9: Time series (a-d) of the Loco Swarm avoiding collision as an operator walks through the center of the flight volume. The △ symbol denotes the position of the operator, while the ○ symbols denote the agents in the swarm. Both the operator and the agents are shown with their respective repulsive radii of influence. The × symbols represent the assigned goal locations for the agents.

REFERENCES

[1] C. Carbone, O. Garibaldi, and Z. Kurt, "Swarm robotics as a solution to crops inspection for precision agriculture," *KnE Engineering*, vol. 3, pp. 552–562, 2 2018.

[2] J. Chen, M. Gauci, W. Li, A. Kolling, and R. Groß, "Occlusion-based cooperative transport with a swarm of mobile robots," *IEEE Transactions on Robotics*, vol. 31, pp. 307–321, 4 2015.

[3] G. A. Cardona, J. Ramirez-Rugeles, E. Mojica-Nava, and J. M. Calderon, "Visual victim detection and quadrotor-swarm coordination control in search and rescue environment," *International Journal of Electrical and Computer Engineering*, vol. 11, pp. 2079–2089, 6 2021.

[4] G. Quiroz and S. J. Kim, "A confetti drone: Exploring drone entertainment," in *2017 IEEE International Conference on Consumer Electronics (ICCE)*. IEEE, 3 2017, pp. 378–381.

[5] M. Sigalas, H. Baltzakis, and P. Trahanias, "Gesture recognition based on arm tracking for human-robot interaction," in *2010 IEEE/RSJ International Conference on Intelligent Robots and Systems (IROS)*. IEEE, 12 2010, pp. 5424–5429.

[6] M. A. Kassab, M. Ahmed, A. Maher, and B. Zhang, "Real-time human-uav interaction: New dataset and two novel gesture-based interacting systems," *IEEE Access*, vol. 8, pp. 195 030–195 045, 10 2020.

[7] J. Nagi, F. Ducatelle, G. A. D. Caro, D. Cireşan, U. Meier, A. Giusti, F. Nagi, J. Schmidhuber, and L. M. Gambardella, "Max-pooling convolutional neural networks for vision-based hand gesture recognition," in *2011 IEEE International Conference on Signal and Image Processing Applications (ICSIP)*. IEEE, 11 2011, pp. 342–347.

[8] J. Nagi, A. Giusti, L. M. Gambardella, and G. A. D. Caro, "Human-swarm interaction using spatial gestures," in *2014 IEEE International Conference on Intelligent Robots and Systems (IROS)*. IEEE, 9 2014, pp. 3834–3841.

[9] A. Chaudhary, T. Nascimento, and M. Saska, "Controlling a swarm of unmanned aerial vehicles using full-body k-nearest neighbor based action classifier," in *2022 International Conference on Unmanned Aircraft Systems, (ICUAS)*. IEEE, 6 2022, pp. 544–551.

[10] B. Gromov, J. Guzzi, L. M. Gambardella, and A. Giusti, "Intuitive 3d control of a quadrotor in user proximity with pointing gestures," in *2020 IEEE International Conference on Robotics and Automation (ICRA)*. IEEE, 5 2020, pp. 5964–5971.

[11] A. Suresh and S. Martínez, "Human-swarm interactions for formation control using interpreters," *International Journal of Control, Automation and Systems*, vol. 18, pp. 2131–2144, 8 2020.

[12] S. Nagavalli, M. Chandarana, K. Sycara, and M. Lewis, "Multi-operator gesture control of robotic swarms using wearable devices," in *Proceedings of the Tenth International Conference on Advances in Computer-Human Interactions*. IEEE, 2017, pp. 25–33.

[13] J. DelPreto and D. Rus, "Plug-and-play gesture control using muscle and motion sensors," in *Proceedings of the 2020 ACM/IEEE International Conference on Human-Robot Interaction*, 3 2020, pp. 439–448.

[14] B. Gromov, L. M. Gambardella, and G. A. D. Caro, "Wearable multimodal interface for human multi-robot interaction," in *2016 IEEE International Symposium on Safety, Security and Rescue Robotics (SSRR)*. IEEE, 10 2016, pp. 240–245.

[15] L. Overmeyer, F. Podszus, and L. Dohrmann, "Multimodal speech and gesture control of agvs, including eeg-based measurements of cognitive workload," *CIRP Annals - Manufacturing Technology*, vol. 65, pp. 425–428, 1 2016.

[16] M. Chen, P. Zhang, Z. Wu, and X. Chen, "A multichannel human-swarm robot interaction system in augmented reality," *Virtual Reality and Intelligent Hardware*, vol. 2, pp. 518–533, 12 2020.

[17] D. Lee, A. Franchi, H. I. Son, C. Ha, H. H. Bulthoff, and P. R. Giordano, "Semiautonomous haptic teleoperation control architecture of multiple unmanned aerial vehicles," *IEEE/ASME Transactions on Mechatronics*, vol. 18, pp. 1334–1345, 5 2013.

[18] H. I. Son, L. L. Chuang, J. Kim, and H. H. Bülthoff, "Haptic feedback cues can improve human perceptual awareness in multi-robots teleoperation," in *2011 International Conference on Control, Automation and Systems (ICCAS)*. IEEE, 10 2011, pp. 1323–1328.

[19] M. MacChini, T. Havy, A. Weber, F. Schiano, and D. Floreano, "Hand-worn haptic interface for drone teleoperation," in *2020 IEEE International Conference on Robotics and Automation (ICRA)*, 5 2020, pp. 10 212–10 218.

[20] E. Tsykunov, R. Agishev, R. Ibrahimov, L. Labazanova, A. Tleugazy, and D. Tsetserukou, "Swarmtouch: Guiding a swarm of micro-quadrotors with impedance control using a wearable tactile interface," *IEEE Transactions on Haptics*, vol. 12, pp. 363–374, 7 2019.

[21] Q. Ouyang, J. Wu, and M. Wu, "Vibrotactile display of flight attitude with combination of multiple coding parameters," *Applied Sciences*, vol. 7, 12 2017.

[22] N. Shibata, S. Sugiyama, and T. Wada, "Collision avoidance control with steering using velocity potential field," in *Proceedings of the 2014 IEEE Intelligent Vehicles Symposium*. IEEE, 6 2014, pp. 438–443.

[23] M. T. Wolf and J. W. Burdick, "Artificial potential functions for highway driving with collision avoidance," *Proceedings - IEEE International Conference on Robotics and Automation*, pp. 3731–3736, 2008.

[24] H. Hongyu, Z. Chi, S. Yuhuan, Z. Bin, and G. Fei, "An improved artificial potential field model considering vehicle velocity for autonomous driving," *IFAC-PapersOnLine*, vol. 51, no. 31, pp. 863–867, 1 2018.

[25] Y. Yan and Y. Zhang, "Collision avoidance planning in multi-robot based on improved artificial potential field and rules," in *Proceedings of the 2008 IEEE International Conference on Robotics and Biomimetics (ROBIO)*. IEEE, 2 2009, pp. 1026–1031.

[26] J. Sun, J. Tang, and S. Lao, "Collision avoidance for cooperative uavs with optimized artificial potential field algorithm," *IEEE Access*, vol. 5, pp. 18 382–18 390, 8 2017.

[27] D. J. Bennet and C. R. McInnes, "Distributed control of multi-robot systems using bifurcating potential fields," *Robotics and Autonomous Systems*, vol. 58, pp. 256–264, 3 2010.

[28] H. Gaber, S. Amin, and A.-B. M. Salem, "A combined coordination technique for multi-agent path planning," in *2010 International Conference on Intelligent Systems Design and Applications*. IEEE, 11 2010, pp. 563–568.

[29] Y. Emam, P. Glotfelter, and M. Egerstedt, "Robust barrier functions for a fully autonomous, remotely accessible swarm-robotics testbed," in *Proceedings of the 2019 IEEE Conference on Decision and Control (CDC)*. IEEE, 12 2019, pp. 3984–3990.

[30] X. Zhang, X. Chen, Y. Li, V. Lantz, K. Wang, and J. Yang, "A framework for hand gesture recognition based on accelerometer and emg sensors," *IEEE Transactions on Systems, Man, and Cybernetics-Part A: Systems and Humans*, vol. 41, pp. 1064–1076, 3 2011.

[31] "gforcepro+ emg armband," 2021. [Online]. Available: http://www.oymotion.com/en/product32/149

[32] "Loco swarm bundle," 2021. [Online]. Available: https://store.bitcraze.io/products/the-swarm-bundle

[33] "Crazyflie 2.1," 2021. [Online]. Available: https://store.bitcraze.io/products/crazyflie-2-1

[34] "Loco positioning system," 2021. [Online]. Available: https://www.bitcraze.io/documentation/system/positioning/loco-positioning-system/

[35] "Loco positioning node," 2021. [Online]. Available: https://store.bitcraze.io/products/loco-positioning-node

[36] "Loco positioning deck," 2021. [Online]. Available: https://store.bitcraze.io/products/loco-positioning-deck

[37] J. A. Preiss, W. Honig, G. S. Sukhatme, and N. Ayanian, "Crazyswarm: A large nano-quadcopter swarm," in *Proceedings of the 2017 IEEE International Conference on Robotics and Automation (ICRA)*. IEEE, 7 2017, pp. 3299–3304.

[38] 2021. [Online]. Available: https://www.bhaptics.com/tactsuit/tactsuit-x40

[39] D. Hernández, J. M. Cecília, C. T. Calafate, J.-C. Cano, and P. Manzoni, "The kuhn-munkres algorithm for efficient vertical takeoff of uav swarms," in *2021 IEEE Vehicular Technology Conference (VTC2021-Spring)*. IEEE, 4 2021, pp. 1–5.

[40] Z. Zhang, K. Yang, J. Qian, and L. Zhang, "Real-time surface emg pattern recognition for hand gestures based on an artificial neural network," *Sensors*, vol. 19, pp. 1–16, 7 2019.

[41] P. B. Shull, S. Jiang, Y. Zhu, and X. Zhu, "Hand gesture recognition and finger angle estimation via wrist-worn modified barometric pressure sensing," *IEEE Transactions on Neural Systems and Rehabilitation Engineering*, vol. 27, pp. 724–732, 4 2019.

[42] O. Khatib, "Real-time obstacle avoidance for manipulators and mobile robots," *The International Journal of Robotics Research*, vol. 5, pp. 90–98, 3 1986.